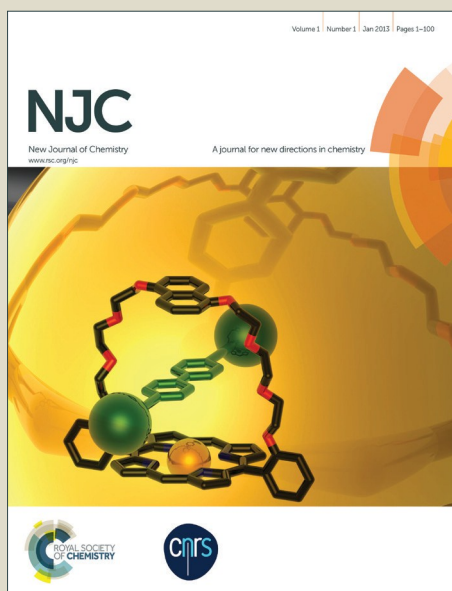


NJC

Accepted Manuscript



This article can be cited before page numbers have been issued, to do this please use: K. Rajavelu, P. Rajakumar, S. Mandal and K. Ramanujam, *New J. Chem.*, 2016, DOI: 10.1039/C6NJ02126C.



This is an *Accepted Manuscript*, which has been through the Royal Society of Chemistry peer review process and has been accepted for publication.

Accepted Manuscripts are published online shortly after acceptance, before technical editing, formatting and proof reading. Using this free service, authors can make their results available to the community, in citable form, before we publish the edited article. We will replace this *Accepted Manuscript* with the edited and formatted *Advance Article* as soon as it is available.

You can find more information about *Accepted Manuscripts* in the [Information for Authors](#).

Please note that technical editing may introduce minor changes to the text and/or graphics, which may alter content. The journal's standard [Terms & Conditions](#) and the [Ethical guidelines](#) still apply. In no event shall the Royal Society of Chemistry be held responsible for any errors or omissions in this *Accepted Manuscript* or any consequences arising from the use of any information it contains.

Synthesis, photophysical, electrochemical and DSSC application of novel donor-acceptor triazole bridged dendrimers with triphenylamine core and benzoheterazole as surface unit

Kannan Rajavelu,^a Perumal Rajakumar,^{*a} Mandal Sudip^b and Ramanujam Kothandaraman^b

^aDepartment of Organic Chemistry, University of Madras, Guindy Campus, Chennai 600 025, Tamilnadu, India and ^bDepartment of Chemistry, Indian Institute of Technology Madras, Chennai-600 036, India.

*Corresponding Author: Tel No: +91 44 2220 2810; E-Mail: Perumalrajakumar@gmail.com

Abstract:

Triazole bridged novel donor-acceptor dendrimers with triphenylamine as core and benzoheterazole as surface unit has been synthesized by click chemistry via convergent approach. All the dendrimers exhibited excellent optical and electrochemical properties, supported by DFT calculations. Lower-generation dendrimers exhibit better current generating capacity and also shows better power conversion efficiency than higher-generation dendrimers when used as additives in dye-sensitized solar cells.

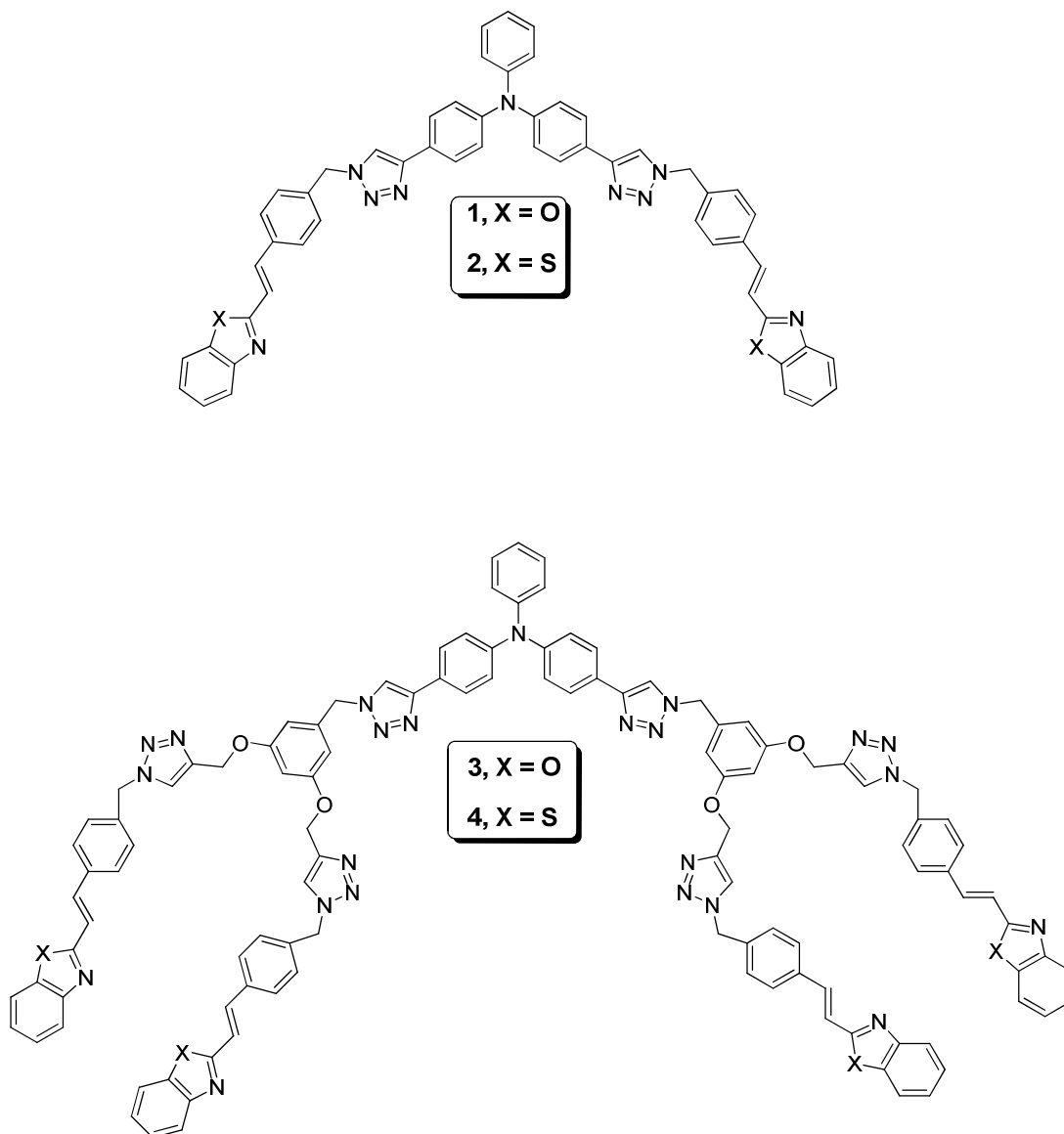
Introduction

The development of new organic materials for the application in molecular organic electronics,¹ nanotechnology,² and optoelectronic devices³ such as organic solar cells and organic light emitting diodes have shown a remarkable scientific activity due to their relevance in the generation and rational use of energy. Great challenge to the research community to prepare low cost renewable energy sources could also find a niche as power supplies in the emerging area of flexible optoelectronics. With more recent development, dendrimers are used as hole transporting material in electronics. Dendrimers are mono dispersed macromolecules

possessing well-defined structure that can be precisely tailored with discrete functionalities to create multifunctional materials. These molecules, with highly branched globular three-dimensional architecture, present multiple chains emanating from a single core. Challenges in the field of dendrimers lie in the synthesis using modern techniques and most frequently in the purification of the synthesized nano molecules. Dendrimers have been extensively used in pioneering work by Vögtle, Tomalia, Fréchet and Newkome⁴. Dendrimers have received much attention in the areas of material science and biological science such as in versatile biomimetic catalysis, drug delivery systems,⁵ sensors, solar cell additives⁶ and efficient light harvesting antenna, multivalent diagnostics for magnetic resonance imaging (MRI),⁷ molecular encapsulation and in bio-conjugate chemistry.⁸ Recent work in this area focus on the synthesis of new donor-acceptor dendrimers with triazole bridging unit. If such system has an efficient electron transfer from donor to acceptor upon photo-excitation of the sensitizer, the negative charge accumulated on the acceptor can be injected into the conduction band (CB) of a metal oxide semiconductor.⁹ Such supramolecular architecture with combined donor and acceptor blocks can reduce band gap energy also. Triphenylamine is an excellent electron-donating group with aggregation-resistant and nonplanar molecular shape which makes it as an important donor in many systems.¹⁰ Organic glasses can be derived from highly electron donating triphenylamine derivatives.¹¹ Many factor plays an important role in increasing the energy harvesting efficiency of triphenylamine dendrimers by intramolecular charge transfer (ICT),¹² molecular coplanarity, vibronic coupling, good stability to oxidation and charge carrier mobility. Triphenylamine possesses a propeller shaped, electron rich structure¹³ which can maintain uninterrupted conjugation with the help of lone pair of electrons at the central nitrogen atom, to enhance the electronic communication along with macromolecular chains and make them to behave as strong

electron donor, and radical cations that help to enhance electrical or photochemical stabilities for charge transfer from the donor to acceptor.¹⁴ Two electron acceptors can be introduced into the organic donor viz: triphenylamine framework. The two electron acceptor groups can affect not only the absorption spectra or molar extinction coefficients and also the HOMO and LUMO levels of the sensitizers. Research efforts to increase the power conversion efficiency in DSSC using nitrogen containing heterocycles such as pyrazole, imidazole, triazole, pyridine, pyrimidine, and pyrazine as additives show an increase in the V_{oc} value and improve the efficiency.¹⁵ In 1991 Michael Gratzel and Brian O'Regan reported DSSC capable of 10% energy conversion efficiency.¹⁶ Unlike ruthenium sensitizers N719 or N3 is commonly employed in DSSCs and most of the triphenylamine dye possess one single group for TiO_2 grafting. From the literature survey, there is no report on the synthesis of dendrimers through click chemistry with benzoheterazole unit as attractive acceptor at periphery with electron donating triphenylamine unit as the central core in order to study their application in material chemistry and biology. Thus, to fully explore the potential of the benzoheterazole¹⁷ unit, synthesis of such novel class of molecule is highly desirable. Benzoheterazole has interesting biological applications such as anticonvulsant, anticancer, anti-HIV, antidiabetic, antialzheimer, antihypertensive and antioxidant properties.¹⁸ Nowadays, click chemistry has emerged as an efficient tool for the rapid synthesis of triazole bridged dendrimers via Cu (I)-catalyzed Huisgen 1,3-dipolar cycloaddition introduced by Sharpless and co-workers which has been widely used in the design and synthesis of optoelectronic materials and affords a good way to achieve target molecules under mild reaction conditions with high efficiency.¹⁹ Generally, click chemistry provides excellent regioselectivity and high yield without any side reactions. Recently, we have used dendrimers as additives to improve the efficiency of DSSCs. In our laboratory dendrimers with

dimethyl isophthalate²⁰ and pyrene²¹ at the periphery has been used as additive in DSSCs. The present investigation mainly focus on the synthesis and photophysical, electrochemical properties and DSSCs application of dendrimers **1-8** having benzoheterazole surface group (Fig.1).



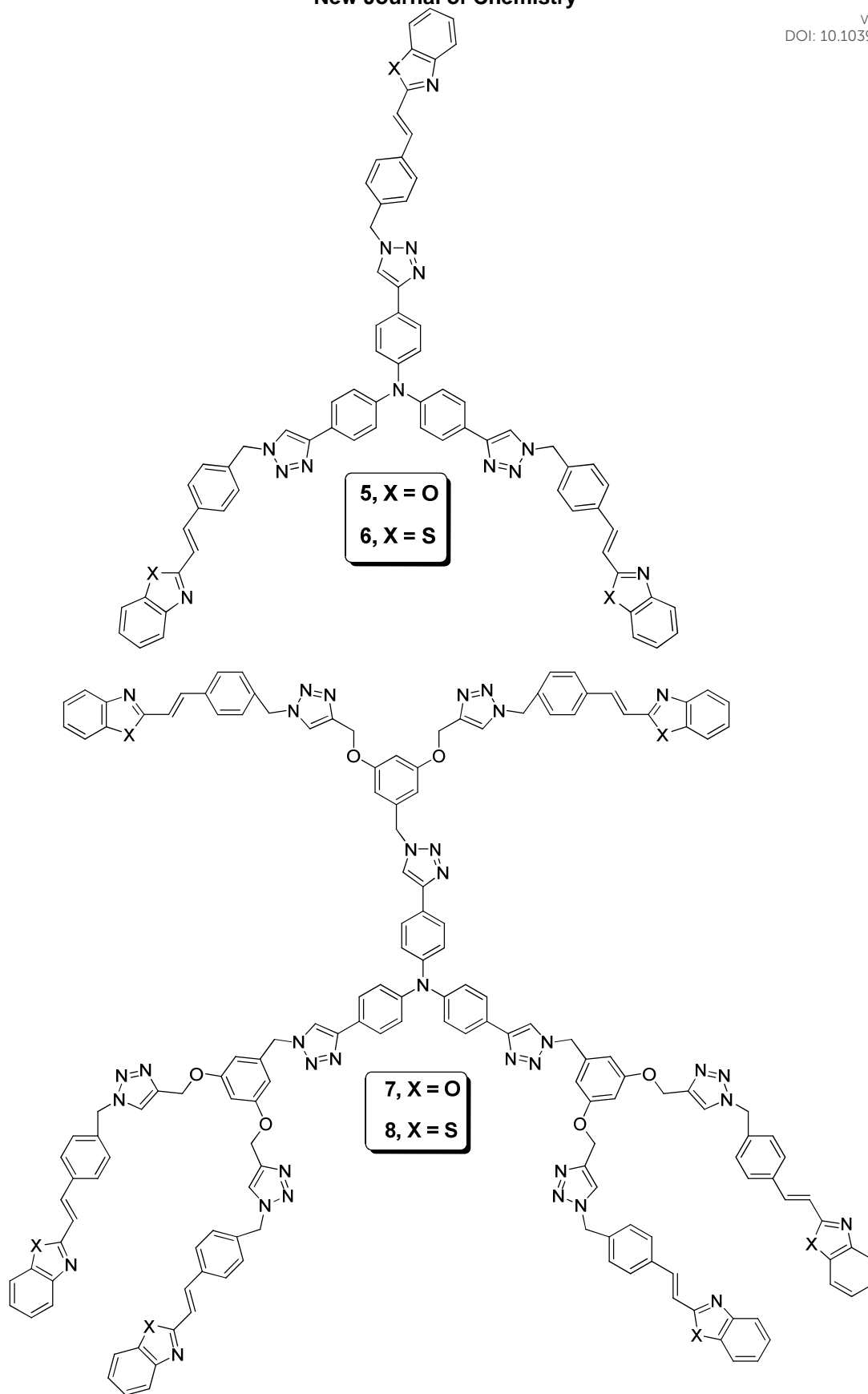


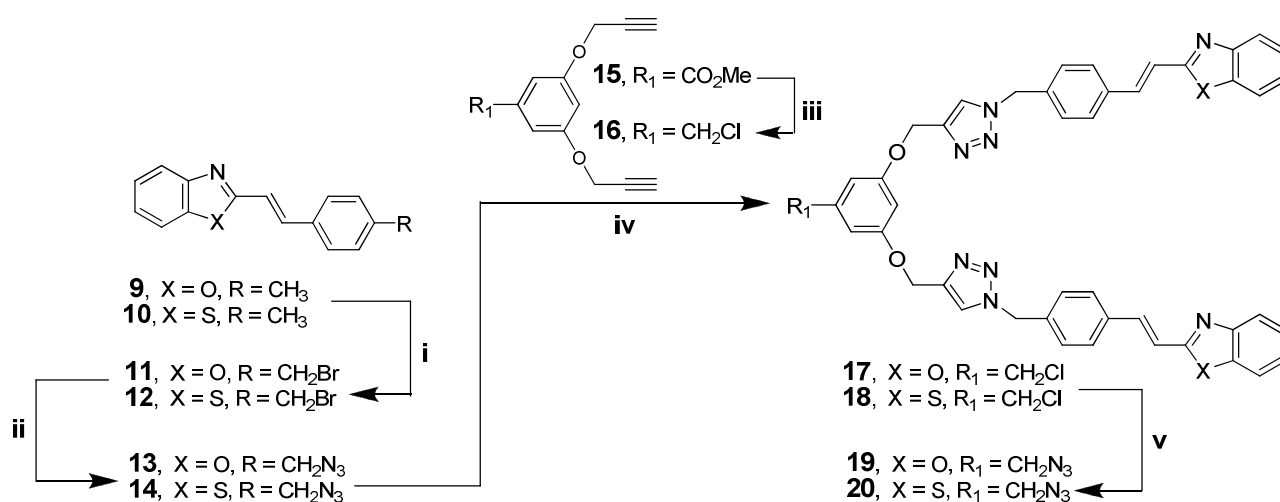
Fig. 1 Molecular structure of benzoheterazole dendrimers 1-8

Results and discussion

In order to explore the utility of benzoheterazole as a surface unit in dendrimers, the dendritic wedge **13** and **14** were synthesized as outlined in **Scheme 1**. Our synthesis starts from the reaction of 4-methyl cinnamic acid with 2-aminophenol /2-amino thiophenol in POCl₃ at 100 °C for 5 h to give 2-[4-(methyl)styryl]benzoxazole **9** and 2-[4-(methyl)styryl]benzothiazole **10** in **85%** and **90%** yields, respectively. In the ¹H NMR spectrum 2-(4-(methyl)styryl)benzothiazole **10**, the olefinic hydrogens are cis to each other due to twisted intramolecular charge transfer from donor 4-methylbenzene and acceptor benzothiazole and also hydrogen bonding interaction in the presence of polar solvents changes the geometry from trans to cis form in benzothiazole.²² The bromides **11** and **12** were obtained in **65%** and **70%** yields by the reaction of 2-[4-(methyl)styryl]benzoheterazole **9** and **10** with NBS. Azidation of **11** and **12** with 1.2 equiv. of NaN₃ in a mixture of acetone/H₂O (4:1) at 60 °C for 6 h gave the azides **13** and **14** in **91%** and **89%** yields, respectively.

We then focused our attention on the synthesise of the first generation dendritic chlorides, the building unit viz. 3,5-bis(propargyloxy)benzyl chloride **16**, was obtained as follows: the bis-propargyl derivative **15** was obtained by the reaction of methyl 3,5-dihydroxybenzoate with propargyl bromide in dry DMF in the presence of K₂CO₃ followed by reduction with LiAlH₄ to give the corresponding alcohol which was then reacted with SOCl₂/ Py in DCM to give 3,5-bis(propargyloxy)benzyl chloride **16**. Reaction of the chloride **16** with 2.1 equiv. of 2-[4-(azidomethyl)styryl]benzoheterazole **13** and **14** under the click reaction conditions viz., CuSO₄.5H₂O and sodium ascorbate in a 1 : 1 mixture of t-BuOH and water at room temperature afforded first generation dendritic chlorides (G1-Cl) **17** and **18** in **90%** and **87%** yields, respectively. In the ¹H NMR spectrum dendritic chloride **17** displayed three sets of

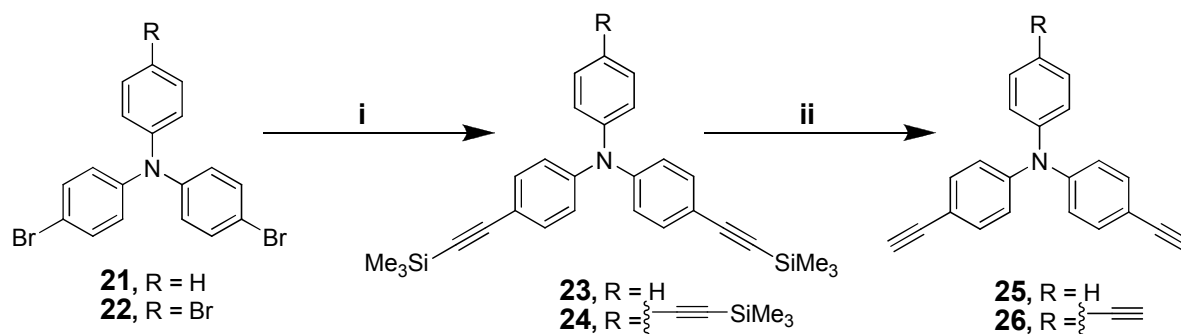
singlets at δ 4.47, 5.16 and 5.55 for benzylic chloromethane, *N*-methylene and *O*-methylene protons respectively, in addition to the signals for the aromatic protons. In the ^{13}C NMR spectrum **17** showed signals at δ 46.0, 53.8 and 62.1 for benzylic chloromethane, *N*-methylene and *O*-methylene carbons respectively, in addition to the signals for the aromatic carbons. The dendritic chloride **17** and **18** was further converted into the first generation dendritic azides (G1- N_3) **19** and **20** in **87%** and **86%** yields, respectively by the reaction of the chloride **17** and **18** with 1.2 equiv. of NaN_3 in DMF at room temperature for 24 h.



Scheme 1: (i) 1.2 equiv. *N*-Bromosuccinimide, benzoyl peroxide, benzene, 60 °C, 8 h. (ii) 1.5 equiv. sodium azide, acetone/water (4:1), 60 °C, 4 h. (iii) LAH, THF, rt then followed by SOCl_2/Py . (iv) $\text{CuSO}_4 \cdot 5\text{H}_2\text{O}$ (5 mol %), NaAsc (10 mol %), THF/ H_2O (1:1), rt, 12 h. (v) 1.2 equiv. sodium azide, DMF, rt, 24 h.

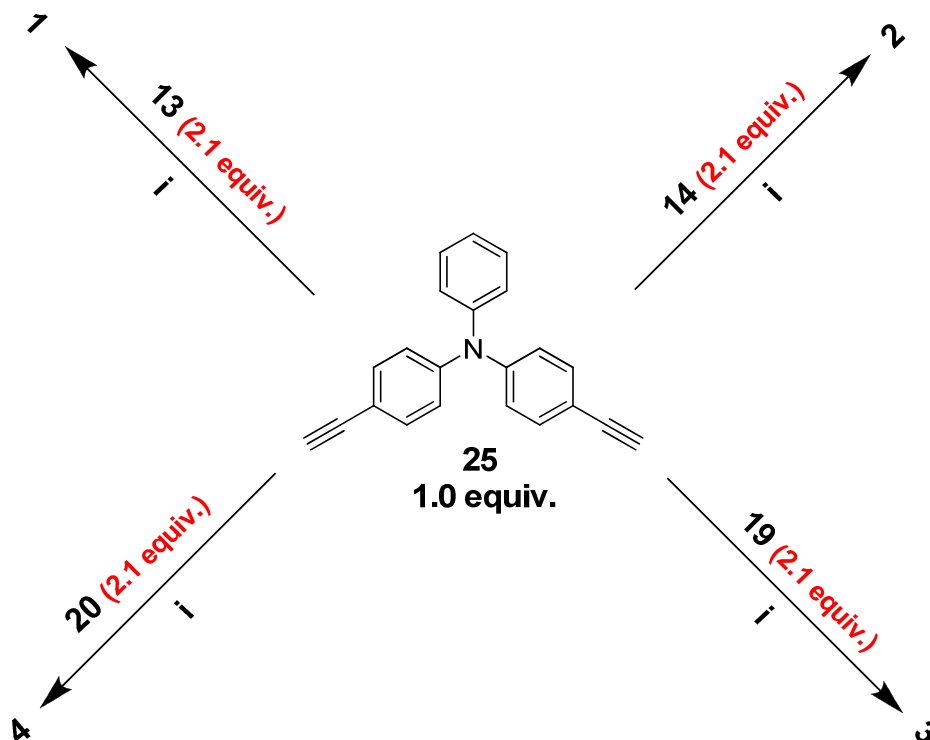
The core unit diyne **25** and triyne **26** can be synthesized by multi-step procedure as reported in the literature²³. via simple bromination of triphenylamine with 2.1/3.1 equivalents of *N*-bromosuccinimide in DMF followed by Sonogashira coupling of 3.0/4.5 equivalents of

trimethylsilylacetylene in a mixture of THF/Et₃N to give the bis silylated acetylene **23** and tris silylated acetylene **24** in **70%** and **82%** yields, respectively. Removal of TMS protecting group using K₂CO₃ in methanol gave the diyne **25** and the triyne **26** in **90%** and **80%** yields, respectively (**Scheme 2**).



Scheme 2: (i) 3.0 equiv. / 4.5 equiv. trimethylsilylacetylene, 6% [PdCl₂(PPh₃)₂], 3% PPh₃, 3% CuI, Et₃N/THF, 90 °C. (ii) Anhydrous potassium carbonate, methanol, rt, 24 h.

Treatment of 1.0 equiv. of diyne **25** with 2.1 equiv. of 2-(4-(azidomethyl)styryl)benzoheterazole **13** and **14** in the presence of CuSO₄·5H₂O (5 mol%) and sodium ascorbate (10 mol%) in a mixture of THF and H₂O (1:1) at room temperature for 12 h afforded dendrimers **1** and **2** in **65%** and **70%** yields, respectively (**Scheme 3**). In the ¹H NMR spectrum, dendrimer **1** showed a four proton singlet at δ 5.60 for *N*-methylene proton and two proton singlet at δ 7.63 for triazole proton in addition to the signals for aromatic protons. In the ¹³C NMR spectrum, dendrimer **1** displayed *N*-methylene carbon at δ 53.8 in addition to the signals for the aromatic carbons. In the ESI mass spectrum dendrimer, **1** showed a molecular ion peak at *m/z* 846 [M + H]⁺. Similarly, the structure of the zeroth generation dendrimer **2** was also confirmed from spectral and analytical data.

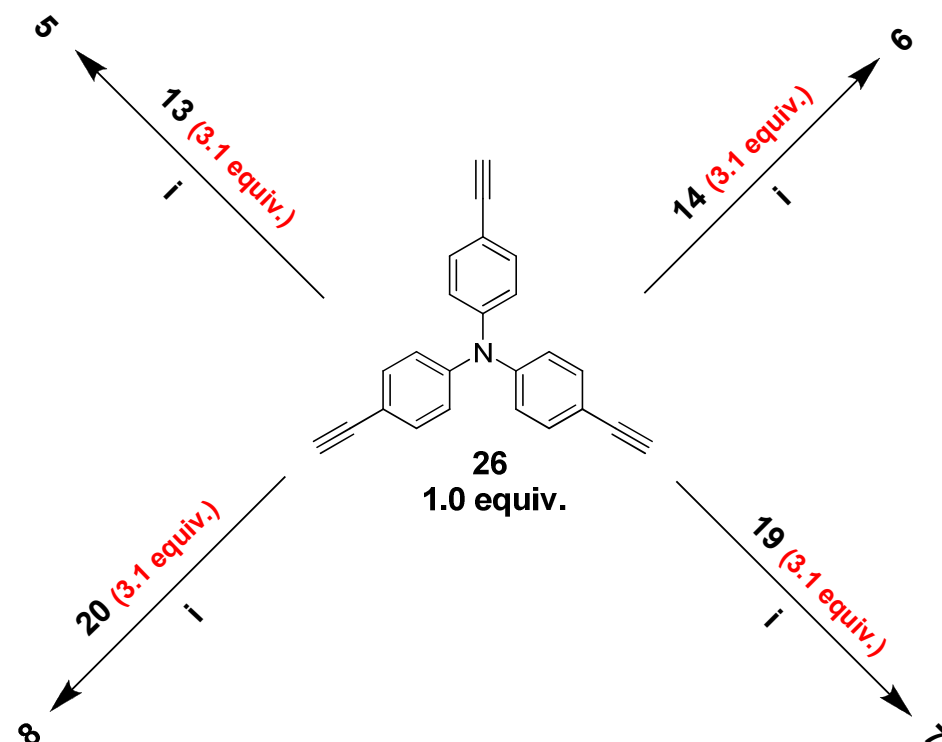


Scheme 3: (i) $\text{CuSO}_4 \cdot 5\text{H}_2\text{O}$ (5 mol%), NaAsc (10 mol%), THF/ H_2O (1:1), rt, 12 h.

In order to synthesize the first generation dendrimers **3** and **4**, 1.0 equiv. of the diyne **25** was reacted with 2.1 equiv. of each dendritic azides **19** and **20** in 5 mol% $\text{CuSO}_4 \cdot 5\text{H}_2\text{O}$ with 10 mol% sodium ascorbate in a mixture of DMF and H_2O (4:1) for 12 h at room temperature to afford the dendrimers **3** and **4** in **58% and 53%** yields, respectively (**Scheme 3**). In the ^1H NMR spectrum, dendrimer **3** displayed three singlets at δ 5.12, 5.53 and 5.62 for two types of benzylic *N*-methylene protons and *O*-methylene proton and two signals at δ 8.30, 8.53 for the triazole protons of two types of triazole ring systems viz: outer, at the dendritic wedge and inner, near the core unit respectively. In the ^{13}C NMR spectrum, dendrimer **3** displayed three signals at δ 52.5, 61.5 and 79.1 for two type's benzylic *N*-methylene carbons and *O*-methylene carbon in addition to the signal for the aromatic carbons. The ESI mass spectrum of **3** showed the molecular ion

peak at m/z 1881 $[M + H]^+$. Similarly the structure of the first generation dendrimer **4** was also confirmed from spectral and analytical data.

The triyne **26** was then utilized for the synthesis of dendrimers **5**, **6**, **7** and **8**. Reaction of 3.1 equiv. of the dendritic wedge **13** with 1 equiv. of the triyne **26** under click chemistry conditions gave the dendrimer **5** in 60% yield (Scheme 4). In the ^1H NMR spectrum, dendrimer **5** showed a six proton singlet at δ 5.62 for N- methylene protons and a three proton singlet at δ 7.80 for triazole protons in addition to the signals for the aromatic protons. In the ^{13}C NMR spectrum, dendrimer **5** displayed N-methylene carbon at δ 52.6 in addition to the signals for the aromatic carbons. The mass spectrum of **5** showed a molecular ion peak at m/z 1146 $[M + H]^+$. Similar method was employed for the synthesis of dendrimer **6**, **7** and **8** in 67%, 55% and 50% yields from 1 equiv. of the triyne **26** with 3.3 equiv. of the dendritic wedge **14**, **19** and **20**, respectively. In the ^1H NMR spectrum, dendrimer **8** displayed three singlets at δ 5.13, 5.54 and 5.61 two types of benzylic N-methylene protons and O-methylene protons, a singlet corresponding to six protons at δ 7.59 for the triazolyl protons at the dendritic wedge adjacent to the benzothiazole unit and a singlet corresponding to three protons at δ 8.53 for the triazolyl protons near to the core unit in addition to the signals for aromatic protons. In the ^{13}C NMR spectrum, dendrimer **8** displayed three signals at δ 52.5, 61.1 and 79.0 for two types of N-methylene and one type of O-methylene carbons in addition to the signals for aromatic carbons. The ESI mass spectrum of **8** showed the molecular ion peak at m/z 2796 $[M + H]^+$. The elemental composition also supported the molecular formula of the dendrimer **8**. Similarly, spectroscopic and analytical methods were employed to confirm the structure of the dendrimers **6** and **7**.



Scheme 4: (i) $\text{CuSO}_4 \cdot 5\text{H}_2\text{O}$ (5 mol%), NaAsc (10 mol%), DMF/ H_2O (4:1), rt, 24 h.

Investigation on cis-trans isomerization of benzothiazole in polar solvents

The presence of double bond incorporated between the electron donor and electron acceptor can lead to trans to cis isomerization due to twisted intramolecular charge transfer (TICT) state formation. The trans-2-[4-(methyl)styryl]benzothiazole **10** is a push-pull aromatic olefin, which has benzothiazole ring (acceptor) on one side of the olefin bond and 4-methyl benzene ring (donor) on the other side. The donor and acceptor groups are perpendicular to each other in molecular frame. Fayed et al.²⁴ first reported dimethylaminostyrylbenzothiazole (DMASBT) based intramolecular charge transfer in donor and acceptor system evidenced by the increase in the dipole moment. Saha et al.²⁵ also reinvestigated the structure of trans-2-[4-(Dimethylamino)styryl]benzothiazole both experimentally and theoretically proposed that DMASBT emits from TICT state in polar solvents. To determine the high dipole moment in excited state with twisting of 4-methyl benzene ring and thereby getting stabilized in polar solvents (Chloroform-d , Dimethyl sulfoxide- d_6) the trans geometry changes to cis form due to

the interaction of the lone pair of electrons on the nitrogen atom of benzothiazole unit resulting in hydrogen bonding with polar solvents (**Fig. 2**). The dipole moment of their excited state is greater than that of the ground state. Theoretical calculations clearly suggest that HOMO is more localized on the donor 4-methyl benzene ring and the LUMO is localized on the rest of the benzothiazole and there is a minimum overlap between these molecular orbitals. The DFT calculations predict a rotational barrier of 0.34 eV for the conversion of one geometrical isomer to the other as reported earlier by krishnamoorthy et al²². The optimized geometrical parameters for both the cis and trans isomers of **10** are compiled in **Table 1**. The trans form of benzothiazole unit is most stable at room temperature. Further, energy minimization study was carried out and the energy difference between the cis and trans isomer is -6.06 kcal/mol. The energy value of trans is higher than cis value proving that the trans isomer is more stable compared to the cis isomer. This result clearly reveals that the olefinic double bond is only trans, however gets converted to cis form for benzothiazole system alone in the presence of polar solvents.

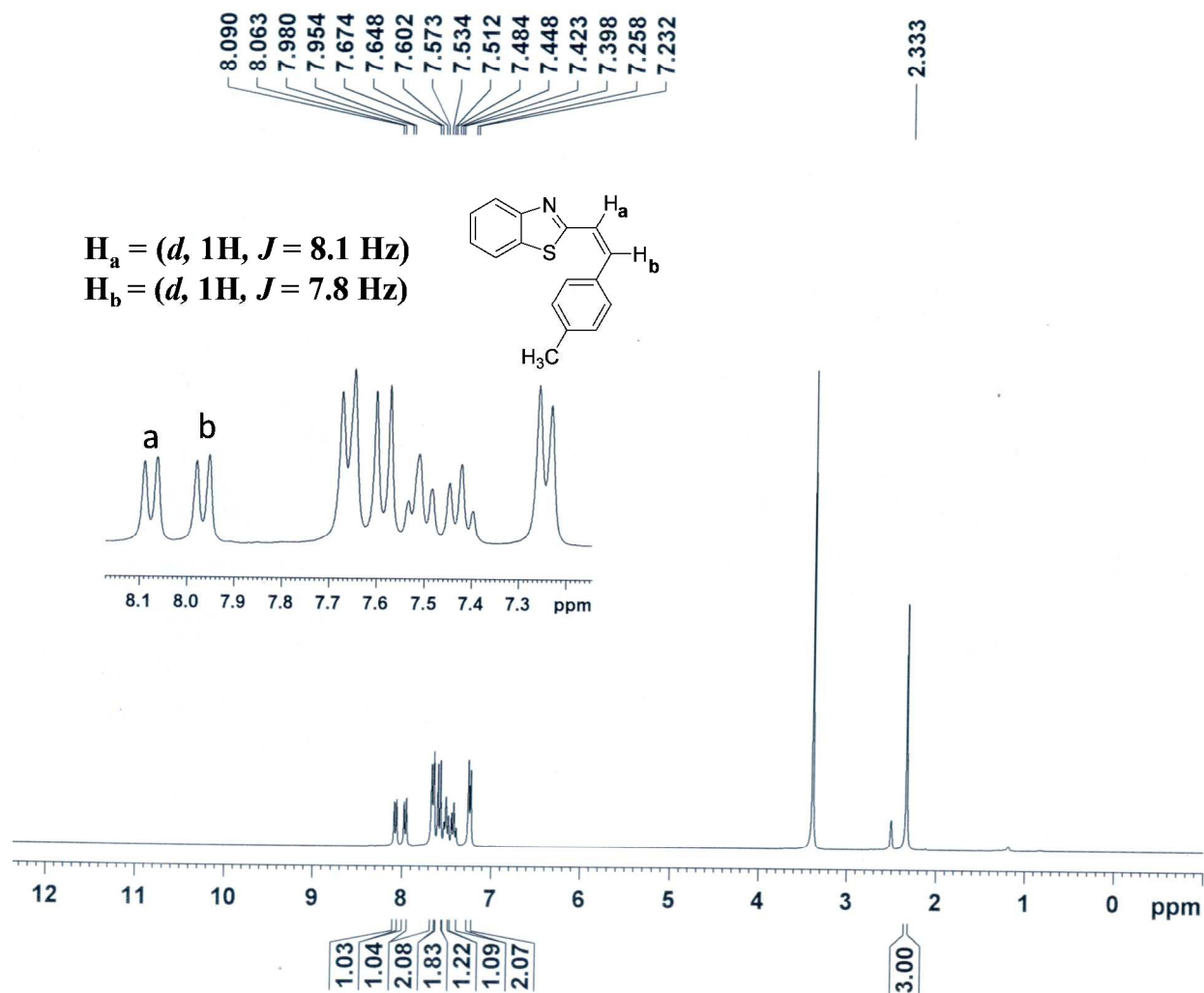


Fig. 2 Shows geometrical changes trans to cis form of benzothiazole group in ^1H NMR spectrum (300 MHz, DMSO- d_6).

Table 1 Frontier molecular energy levels, energy gaps and dipole moments of benzoheterazole molecule.

Molecule	HOMO (eV)	LUMO (eV)	Eg (eV)	Dipole moment μ (Debye)
9 (cis form)	-6.00	-2.05	3.95	2.58
9 (trans form)	-5.91	-2.11	3.80	2.42
10 (cis form)	-6.08	-2.01	4.07	2.33
10 (trans form)	-5.90	-2.18	3.73	1.99

Photophysical studies

The UV-vis absorption and emission spectra of dendrimers **1-8** were recorded in DMF at room temperature and the λ_{max} values are summarized in **Table 2**. Dendrimers **1-8** exhibited strong absorption bands in the range of 324-346 nm. The absorption maxima observed for all the dendrimers could be due to π - π^* transition. The absorption band could be due to the presence of benzoheterazole and donor triphenylamine unit in the molecular system. In fact this observation suggests that both the chromophores involving benzoheterazole and triphenylamine could be responsible for the broad absorption bands for the dendrimers **1-8**. Molar absorption coefficient increases for the bis substituted dendritic wedges with benzoxazole and benzothiazole group as the dendrimer generation increases. The benzoxazole and benzothiazole dendrimers **3** and **4** shows an increase in molar absorption coefficient than that of the zeroth generation benzoxazole and benzothiazole dendrimers **1** and **2** due to valence effect²⁶. However in the case of tris substituted dendritic wedges the molar absorption coefficient decreases for both the benzoxazole

and benzothiazole dendrimer as the dendrimer generation increases from the zeroth to first generation. The molar absorption coefficient of tris substituted benzoxazole dendrimer **7** and tris substituted benzothiazole dendrimer **8** shows decreases in molar absorption coefficient which could be due to excess molecular crowding in tris substituted dendritic wedges. In the fluorescence spectra, the emission values were obtained by exciting all the dendrimers **1-8** at the corresponding absorption maximum. The dendrimers **1-8** exhibited strong fluorescence emission in the region of 388-414 nm and the λ_{em} values for the fluorescence spectra are shown in **Table 2**. The emission spectra showed that the benzoheterazole dendrimers show gradual decrease in emission intensity as the dendrimer generation increases. The decreasing fluorescence intensity is due to fluorescence quenching with increase in number of benzoheterazole unit for self-quenching and the enhancement of non-radioactive transitions.²⁷

Table 2 Photo physical properties of dendrimers **1-8** in DMF (1×10^{-3} mol L⁻¹)

Dendrimer	λ_{max} (nm)	ϵ (mol/L)	λ_{em} (nm)
1	324	571	407
2	344	566	405
3	328	695	388
4	346	675	401
5	328	645	406
6	345	730	406
7	327	625	414
8	339	620	403

Electrochemical studies

The electrochemical property of the benzoheterazole dendrimers **1-8** was studied by recording cyclic voltammetry in DMF at room temperature at a scan rate of 100 mV/s with $n\text{-Bu}_4\text{NPF}_6$ as supporting electrolyte, Glassy carbon electrode as working electrode, Ag/AgCl as reference electrode and Pt electrode as counter electrode. All the synthesized benzoheterazole dendrimers exhibited electrochemical response in cyclic voltammetry and the electrochemical parameters are shown in **Table 3**. The redox behavior of dendrimers **1, 3, 5, 7** and **2, 4, 6, 8** are shown in **Fig. 3a** and **3b**. Oxidation and reduction potential for all the dendrimer appeared in the potential range of -2.0 to +2.0 V. In the cyclic voltammetry two oxidation peaks appeared

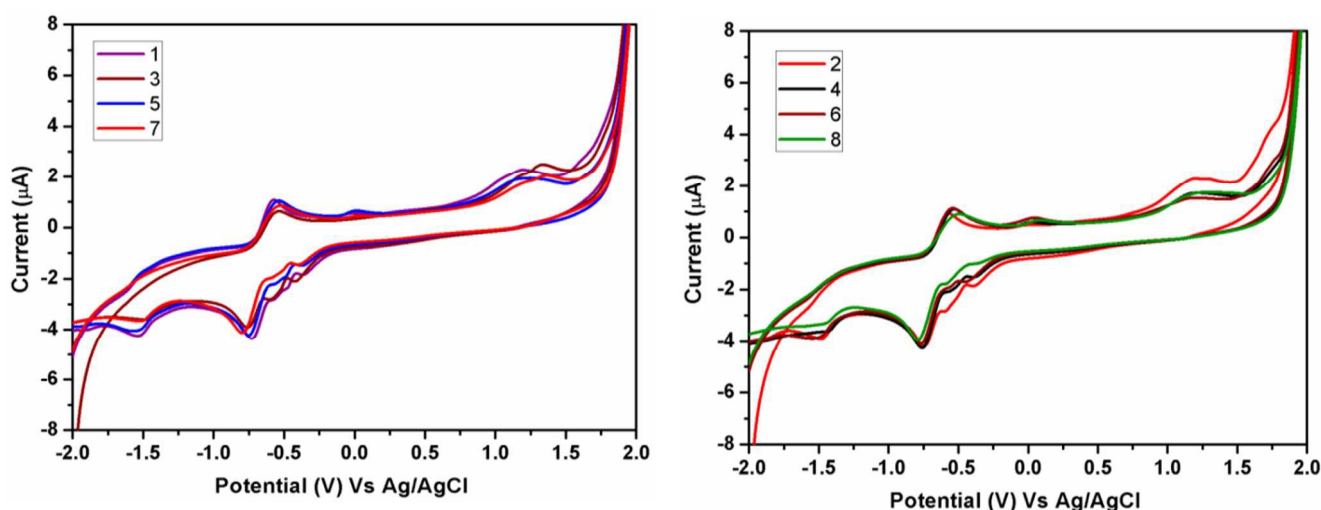


Fig. 3 Cyclic voltammogram of dendrimers a) **1, 3, 5, 7** b) **2, 4, 6, 8** in DMF ($1 \times 10^{-3} \text{ mol L}^{-1}$), scanned at 100 mV s^{-1}

between -1.51 to 1.34 V and two reduction peaks appeared between -0.73 to -1.55 V for all the dendrimers. Oxidation and reduction peaks for all dendrimers **1-8** were attributed to the presence

of strong electron donating triphenylamine and electron withdrawing benzoheterazole groups. All the dendrimer exhibited the first oxidation potential, which is attributed to the oxidation of the triphenylamine core which is quasi reversible²⁸ and benzoheterazole can undergoes quasi reversible single electron transfer process in cathodic scan direction. From the cyclic voltammetry in **Fig. 3a** it is clear that on increasing the number of benzoxazole at periphery, the anodic peak potential which is shifted towards slightly higher positive potential in benzoxazole dendrimer **1, 3, 5** and **7** is due to the presence of triazole and heterocyclic ring. Dendrimers **1, 3, 5** and **7** showed a gradual increase in E_{pa} from 1.20, 1.34, 1.23 and 1.34 V and E_{pc} increases slightly from -0.73, -0.76, -0.75 and -0.81 V. For the benzothiazole dendrimers **2, 4, 6** and **8** there is no potential shift upon increasing the generation growth and anodic peak potential abruptly decreases which could be intramolecular interactions within benzothiazole moiety. The oxidation and reduction potential of the dendrimers from cyclic voltammetry provides strong evidence for the utility of the synthesized molecules in DSSC application.

Table 3 Electrochemical parameters of dendrimers **1-8** in DMF (1×10^{-3} mol L⁻¹)

dendrimer	E_{pa1} (V)	E_{pa2} (V)	E_{pc1} (V)	E_{pc2} (V)	ΔE_{p1} (V)	ΔE_{p2} (V)
1	-0.57	1.20	-0.73	-1.55	0.16	2.75
2	-0.57	1.23	-0.75	-1.48	0.18	2.71
3	-0.55	1.34	-0.76	-1.48	0.21	2.82
4	-0.53	1.22	-0.76	-1.44	0.23	2.66
5	-0.53	1.23	-0.75	-1.54	0.22	2.77
6	-0.55	1.14	-0.78	-1.53	0.23	2.67
7	-0.52	1.34	-0.81	-1.54	0.29	2.88
8	-0.51	1.26	-0.79	-1.47	0.28	2.73

Theoretical calculations

In order to characterize the optical and electronic properties, it is essential to examine the HOMOs, LUMOs, energy gaps and oscillator strength. To gain insight into the molecular structures and electron distribution, the geometries of the triphenylamine containing benzoheterazole unit were fully optimized and the density functional theory calculations was carried out employing the B3LYP/6-31G level with Gaussian 09 programme package.²⁹ Effect of the solvents was simulated by employing DFT calculations using the polarizable continuum model (PCM). As shown in **Fig. 4**, for the zeroth generation dendrimers **1**, **2**, **5** and **6** the excited state LUMO was only localized on a heterocyclic ring and also self charge transfer by the benzoheterazole group is observed. From the HOMO level of the zeroth generation dendrimers **1**, **2**, **5** and **6**, electron density is homogeneously distributed on the electron donor triphenylamine and triazole as linker system. However in the case of dendrimer **1** and **2**, the electron density is distributed to the withdrawing group of phenyl ring due to the conjugation between the phenyl rings in the core unit. It may imply that the planar benzoheterazole blocked by triphenylamine can make electron distribution of HOMO to the electron distribution of the LUMO. The well overlapped HOMO and LUMO orbitals on the linker triazole unit suggest the inductive or withdrawing electron tendency from triphenylamine donor unit to the benzoheterazole unit. Thus, the HOMO and LUMO excitation induced by light irradiation could move the excited electron distribution or charge transfer across the triazole bridge from donor unit to the acceptor unit.³⁰ The oscillator strength can also prove the charge transfer from donor to the periphery and the oscillator strength, excitation energy values support this observation. The frontier molecular orbital of the zeroth generation dendrimers reveals that HOMO-LUMO excitation moves the electron density distribution from the donor triphenylamine to the acceptor benzoheterazole at the periphery through triazole bridging unit (**Table 4**).

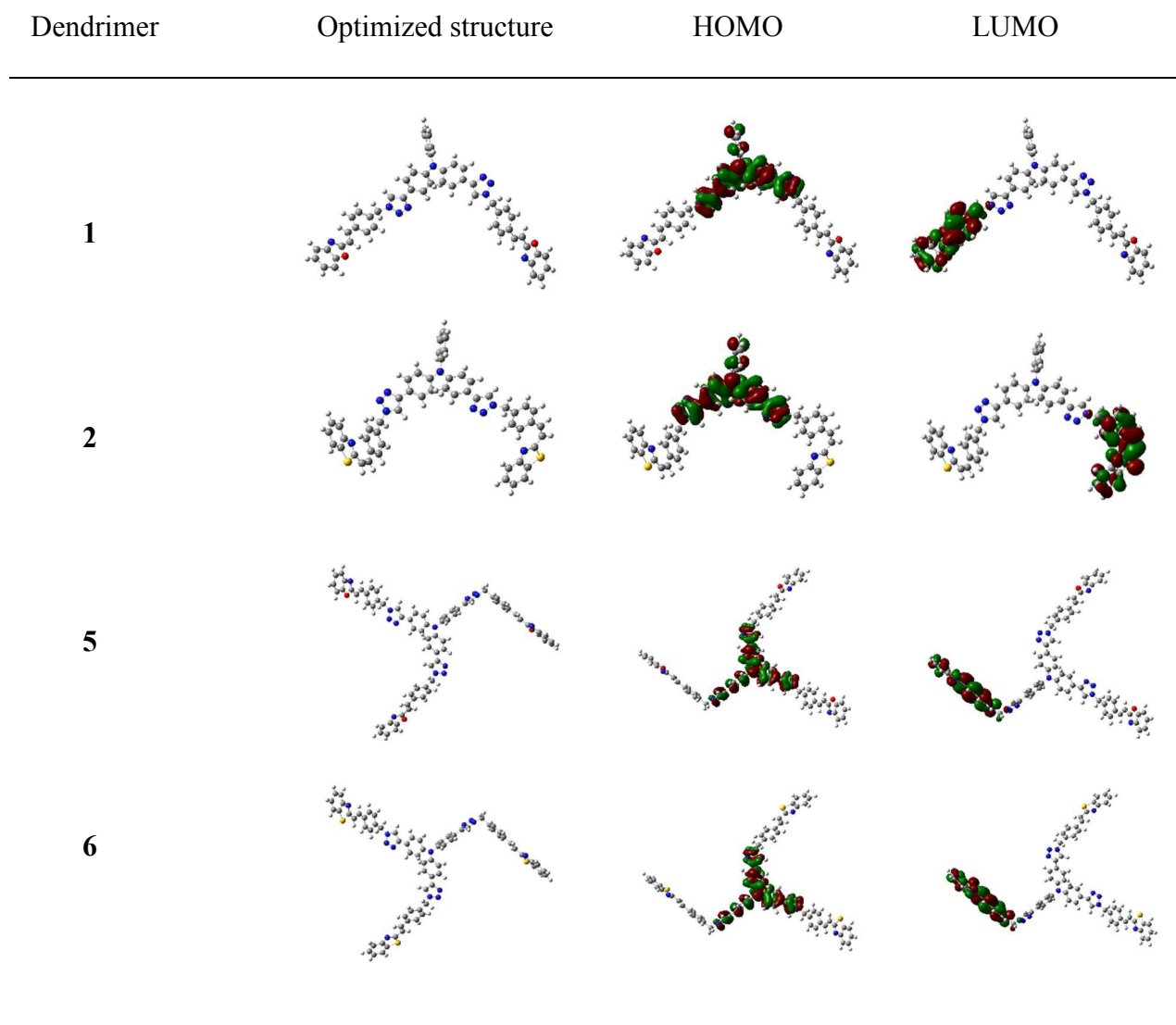


Fig. 4 Frontier molecular orbitals (HOMO and LUMO) of benzoheterazole dendrimer **1**, **2**, **5** and **6** along with the orbital energies obtained at B3LYP/6-311+G(d,p)//6-31G(d,p).

Table 4 Orbital energy levels of benzoheterazole dendrimer **1**, **2**, **5** and **6**

Dendrimer	E _{HOMO} (eV)	E _{LUMO} (eV)	E _g (eV)
1	-5.02	-2.09	2.93
2	-5.02	-2.13	2.89
5	-5.00	-2.08	2.92
6	-4.99	-2.13	2.86

Dye Adsorption on TiO₂ surface

The role of adsorption in device performance is based on the molecular volumes of the dendrimers. In donor-acceptor benzoheterazole dendrimers of higher generation the low efficiency is due to the total amount of dye absorbed on TiO₂ surface³¹ which have a major influence on the solar cell performance and the summarized data are listed in **Table 5**. The higher generation dendrimers **3**, **4**, **7** and **8** can be bind with TiO₂ surface and hence molecular volume of dendrimer increases and also amount of dye absorbed on TiO₂ surface will play important role in solar cell performance in DSSCs. When the generation of the benzoheterazole dendritic acceptor increases the molecular volume of the dyes increase about 2 to 3-fold axis. It is clear that molecular volume or bulkiness of the acceptor moiety plays an important role in the dye uptake.³² Upon increasing from lower to higher generation the molecular volume of acceptor unit increases and the amount of dye uptake decreases in benzoxazole dendrimers with the following order **1** ($3.5 \times 10^{-6} \text{ mol cm}^{-2}$) > **5** ($3.4 \times 10^{-6} \text{ mol cm}^{-2}$) > **3** ($3.1 \times 10^{-6} \text{ mol cm}^{-2}$) > **6** ($3.0 \times 10^{-6} \text{ mol cm}^{-2}$) and also in the case of benzothiazole dendrimers the dye uptake gradually decrease in the following order **2** ($3.3 \times 10^{-6} \text{ mol cm}^{-2}$) > **6** ($3.0 \times 10^{-6} \text{ mol cm}^{-2}$) > **4** ($3.0 \times 10^{-6} \text{ mol cm}^{-2}$) > **8** ($3.0 \times 10^{-6} \text{ mol cm}^{-2}$). As a result in the higher generation dendrimers **3**, **4**, **7** and **8** the amount

of dye adsorption on TiO_2 surface is directly proportional to the high molecular volume of acceptor unit and weak intermolecular π - π interaction.

DSSC studies

Dye sensitized solar cells appear to be highly promising alternatives to more expensive solar cell technologies. The organic nitrogenous compounds have influence on the efficiency of DSSCs which can be explained by the shift of the conduction band potential and the improvement of solar cell performance by the addition of dendrimer additive to the redox

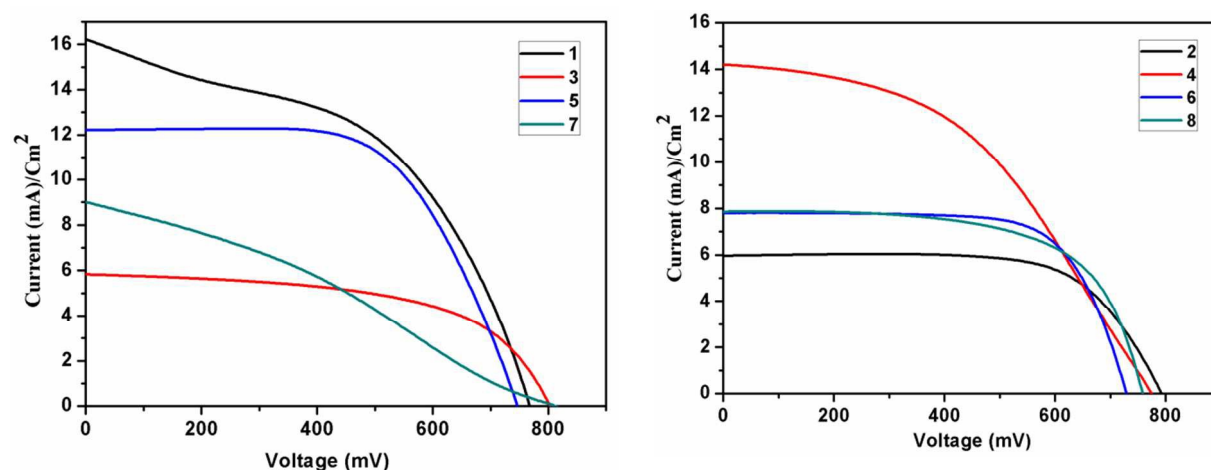


Fig. 5 Current-voltage curves of DSSCs with dendrimer additives (a) **1, 3, 5, 7** (b) **2, 4, 6, 8** in both cases experiments were conducted under simulated solar light at 70 mW cm^{-2} .

electrolyte.³³ Hence, we have planned and synthesized a new type of donor-acceptor triazole dendrimers **1-8** and employed them as additives in DSSCs. **Fig. 5a and 5b** shows the current-voltage (J-V) curves for the undoped electrolyte system and the doped electrolyte system with the benzoheterazole dendrimers **1-8**. The photovoltaic performance of short-circuit current density (J_{sc}), the open-circuit voltage (V_{oc}), and the fill factor and the electric energy efficiency

(η) are summarized in **Table 5**. The present investigations mainly focus on the newly synthesized donor-acceptor triazole bridged dendrimers and the highest power conversion efficiency of **8.02** was observed when the dendrimer **1** was used as an additive in the DSSC. In donor-acceptor dendrimer system on increasing the generation the power conversion efficiency (η) decreases due to aggregation of the dendrimers on the TiO_2 surface which enhance considerably the degree of charge recombination between the injected electrons and the oxidized dendrimers.³⁴ The variation of V_{oc} with increase in generation is mostly associated with charge recombination between the injected electrons in the positive shift of the conduction band and electron acceptor in the electrolyte interface.³⁵ The open circuit current density increases with increasing generation and the power conversion efficiency gradually decreases with benzoxazole dendrimers **1**, **3**, **5** and **7** when used as additive which could be due to back electron transfer to the semiconductor-electrolyte interface.³⁶ In the case of benzothiazole dendrimers **2**, **4**, **6** and **8** the V_{oc} decreases with increasing generation and the power conversion efficiency increases due to cation regeneration and reduce the back current, delocalizing π -electrons on the conjugated donor moiety and the bridged triazole can generate more excited electrons under the same light excitation.³⁷ It is very clear that the photovoltaic performances of the DSSCs can be affected by increasing the generation growth. The number of acceptor unit increases while increasing the generation and the secondary transition progressively gains intensity and shifts to lower energy due to charge transfer from the central donor unit to the two distinct couples of branches which are simultaneously involved in the excitation. An increased dark current by planar organic molecules has been observed by Snaith et al.³⁸ The formation of π -stacked aggregation and self-quenching are the major factors for low conversion efficiency of DSSC.³⁹ The aggregation of the dendrimers may lead to intermolecular quenching or molecules residing in the system that are

not attached to the semiconductor surface.⁴⁰ Therefore, when the dendrimers are anchored on the surface of TiO₂, the LUMO centered on the anchoring moiety should enhance the orbital overlap with the titanium 3d orbital and subsequently favor the electron injection to the conduction band of TiO₂.

Table 5 Photovoltaic performances of DSSCs with doped as well as undoped benzoheterazole dendrimers 1-8 in the electrolyte system (I⁻/I₃⁻) under illumination of 70 mW cm⁻² at AM 1.5 with N719 dye.

DSSC configurations	V_{OC} (mV)	J_{SC} (mA cm ⁻²)	Fill Factor (FF)	Efficiency (η) (%)	Dye loading (moles cm ⁻²)
TiO ₂ /N719/LiI/I ₂ /Pt	792	8.18	0.39	3.60	3.2 x 10 ⁻⁶
TiO ₂ /N719/LiI/I ₂ /1/Pt	764	16.20	0.45	8.02	3.5 x 10 ⁻⁶
TiO ₂ /N719/LiI/I ₂ /2/Pt	791	5.94	0.67	4.51	3.3 x 10 ⁻⁶
TiO ₂ /N719/LiI/I ₂ /3/Pt	801	5.85	0.59	3.97	3.1 x 10 ⁻⁶
TiO ₂ /N719/LiI/I ₂ /4/Pt	774	14.19	0.45	6.80	3.0 x 10 ⁻⁶
TiO ₂ /N719/LiI/I ₂ /5/Pt	745	12.21	0.59	7.63	3.4 x 10 ⁻⁶
TiO ₂ /N719/LiI/I ₂ /6/Pt	731	7.87	0.70	5.80	3.0 x 10 ⁻⁶
TiO ₂ /N719/LiI/I ₂ /7/Pt	811	8.95	0.32	3.22	2.9 x 10 ⁻⁶
TiO ₂ /N719/LiI/I ₂ /8/Pt	757	7.87	0.67	5.70	3.0 x 10 ⁻⁶

Electrochemical impedance spectroscopy

Electrochemical impedance spectroscopy (EIS) is performed to elucidate the interfacial charge recombination processes in DSSCs based on the eight dendrimer additives under dark condition. The Nyquist plot for dendrimer 1-8 are shown in **Fig. 6a and 6b** and the corresponding data are listed in **Table 6**. The Nyquist plots have two semicircles and the larger semicircle at lower frequencies indicates charge recombination resistance at the

TiO₂/dendrimer/electrolyte interface, while the smaller semicircle at higher frequencies corresponds to the charge recombination processes at the Pt/electrolyte interface. The large semicircles, which indicate that charge transfer behavior between TiO₂ and dendrimer electrolytes was significantly due to the increasing surface moiety for higher generation dendrimer.⁴¹ As shown in **Fig. 6a** and **6b** that the radius of the larger semicircle increases for lower generation dendrimers in the order of **1 > 5 > 6 > 2** indicating that the charge recombination resistance gradually increases in zeroth generation dendrimer compared with that of the higher generation dendrimer. The R_{CT} values of benzoxazole dendrimer shows charge transfer resistance for dendrimers in the following order **1 (71.2 Ω) > 5 (56.5 Ω) > 3 (38.6 Ω) > 7 (16.2 Ω)** and also the benzothiazole dendrimer exhibited charge transfer resistance in the following order **2 (13.5 Ω) > 6 (25.3 Ω) > 4 (46.4 Ω) > 8 (21.7 Ω)**. The low R_{CT} value indicates the high charge loss in the TiO₂/electrolyte interface and also faster charge recombination and a larger dark current.⁴² The large value of R_{CT} indicates more effective suppression of the recombination of the injected electron with I^-/I_3^- in the electrolyte.⁴³ Zeroth generation dendrimers **1, 2, 5, and 6** shows a significantly larger charge recombination resistance (R_{CT}) value than the higher generation dendrimers, implying small charge recombination at the TiO₂/electrolyte interface, with a consequent high V_{oc} for the lower generation dendrimers with

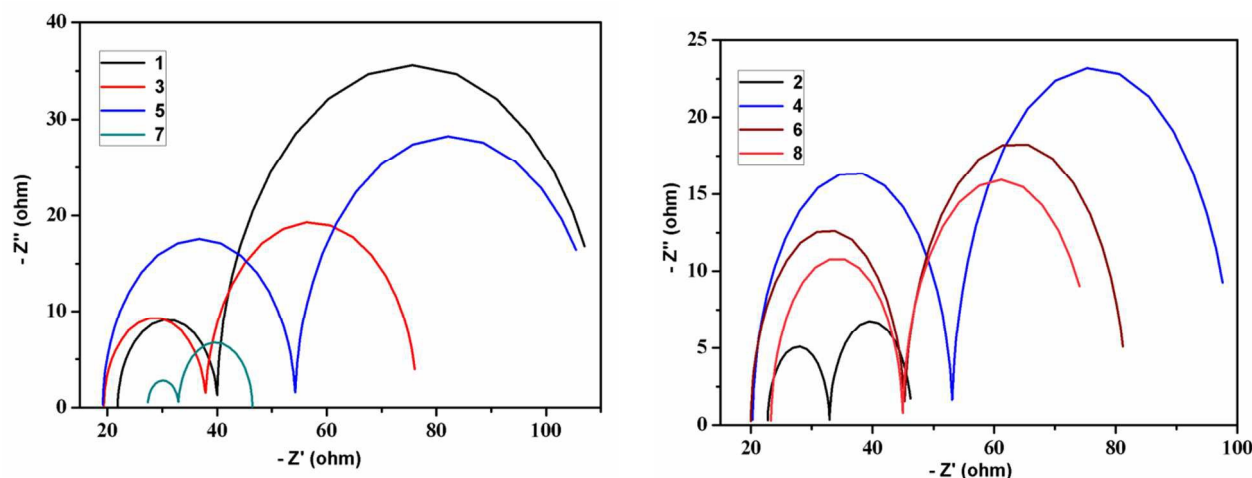


Fig. 6 Electrochemical impedance spectra (Nyquist plot) of the DSSCs a) **1, 3, 5, 7** b) **2, 4, 6, 8** fabricated using with dendrimers measured under dark conditions.

the following order of decreasing V_{oc} is **1** (764 mV) > **5** (745 mV) > **6** (731 mV). The recombination rate caused by backward electron transfer was estimated using the Bode-phase spectra for the DSSCs, as shown in **Fig. 7a** and **7b** and the electron lifetime calculated are shown in **Table 6**. The EIS bode plot exhibits two Bode frequency peaks for electron transfer at the TiO_2 /dendrimer/electrolyte interface and redox charge transfer at the counter electrode. The peak frequency at the lower frequency region is related to the charge recombination rate and the reciprocal is regarded as electron lifetime. The peak at lower frequency corresponds to the large semicircle in the Nyquist plot of dendrimer which is shifted to higher frequency when the molecular volume of higher generation dendrimer increases. On increasing the dendritic

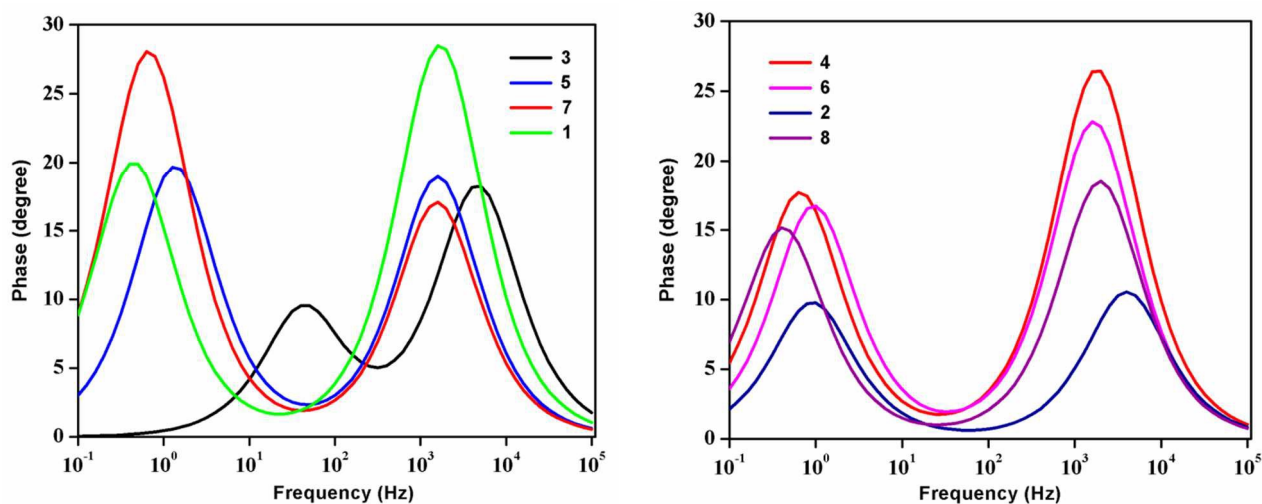


Fig. 7 Electrochemical impedance spectra (Bode plot) of the DSSCs a) **1, 3, 5, 7** b) **2, 4, 6, 8** fabricated using with dendrimers measured under dark conditions.

generation the electron lifetime gradually decrease⁴⁴ which shows that dendrimer **2** (4.8 ms) > **6** (2.2 ms) > **4** (1.6 ms) > **8** (1.4 ms). For the benzothiazole dendrimers **2**, **4**, **6** and **8**, the electron recombination to the I_3^- ions enhance the electron lifetime to confirm the better DSSCs performance. The high molecular volume of dendrimers **3**, **4**, **7** and **8** could not prevent the I_3^- ions reaching the TiO_2 surface, thus leading to the enlarged charge recombination or dark current and shortened electron life time.⁴⁵ It is believed that with maximum amount of dye adsorbed on TiO_2 film and more number of benzoheterazole units in higher generation appear to raise the chances of the electrolyte being close to the TiO_2 surface.

Table 6 Parameters obtained by fitting the electrochemical impedance spectra of the DSSCs with dendrimers 1-8.

dendrimers	R_s (Ω)	R_{CT1} (Ω)	R_{CT2} (Ω)	C_1 (μF)	C_2 (μF)	τ_n (ms)
TiO₂/N719/LiI/I₂/Pt	18.6	6.94	8.14	6.85	516	4.2
TiO₂/N719/LiI/I₂/1/Pt	21.9	71.2	18.2	5.61	76.1	1.3
TiO₂/N719/LiI/I₂/2/Pt	22.7	13.5	10.2	15.4	473	4.8
TiO₂/N719/LiI/I₂/3/Pt	19.4	38.6	18.6	4.33	75.6	1.4
TiO₂/N719/LiI/I₂/4/Pt	20.3	46.4	32.8	7.16	43.8	1.4
TiO₂/N719/LiI/I₂/5/Pt	19.2	56.5	35.1	9.04	45.3	1.5
TiO₂/N719/LiI/I₂/6/Pt	20.0	25.3	36.6	5.74	61.7	2.2
TiO₂/N719/LiI/I₂/7/Pt	18.0	16.2	13.2	2.91	330	4.3
TiO₂/N719/LiI/I₂/8Pt	23.3	21.7	31.8	15.6	51.9	1.6

Conclusions

In conclusion, triphenylamine cored dendrimers with benzoheterazole surface unit and triazole bridging unit were synthesized in high yields by convergent synthetic strategy via click chemistry approach. All the dendrimers exhibited excellent optical and electrochemical properties. The cyclic voltammetric studies reveal that the triphenylamine core unit showed quasireversible behavior. Zeroth generation dendrimers **1** and **5** exhibited better power conversion efficiency of **8.0 %** and **7.6 %**, respectively, when used as additives in DSSC than the control (N719 dye/LiI/I₂) as well as other benzoheterazole dendrimers are used as additives. DSSCs studies clearly revealed that as the number of benzoheterazole and triazole units increases from the zeroth to the first generation dendrimers, the DSSCs performance decreases due to aggregation and back electron transfer to the conduction band of TiO₂. The density functional theory is also supported by optical, electrochemical as well as DSSCs studies. Further studies to increase the efficiency in DSSCs with benzoheterazole dendrimers as additives is underway.

Experimental Section

General Information

All the reagents and solvents were obtained from Sigma Aldrich, Alfa Aesar, Merck and Avra chemical companies. The known products were identified by the comparison of their melting points and spectral data is already reported in the literature. Melting points were uncorrected and were determined using Toshniwal melting point apparatus by the open capillary tube method. The UV-Vis spectra were recorded on a Hitachi U-3210 spectrophotometer. The emission spectra were recorded on a HORIBA JOBIN YVON Fluoromax-4 spectrophotometer.

The ^1H and ^{13}C NMR spectra were recorded on a Bruker 300 MHz NMR spectrometer. The chemical shifts are reported in ppm (δ) with TMS as an internal standard and the coupling constants (J) are expressed in Hz. Elemental analyses were performed on a Perkin-Elmer 240B elemental analyzer. Electrochemical studies were carried out on a CH Instrument electrochemical analyzer. Electrospray ionization mass spectrometry (ESI-MS) spectra were measured with a LCQ AD mass spectrometer. The Gaussian 09 package was used for Density functional theory (DFT) calculations and their using the polarizable continuum model (PCM). Current-voltage (I-V) measurement was performed using Metrohm Autolab 302N potentiostat/galvanostat with FRA32M module controlled by NOVA 1.10 software.

Fabrication and Characterization of DSSCs

The nanocrystalline TiO_2 photoelectrode was prepared as described earlier.⁴⁶ The prepared TiO_2 electrodes were immersed in a 1mM solution of the sensitized dye Di-tetrabutylammonium cis-bis(isothiocyanato)bis(2,2'-bipyridyl-4,4'-dicarboxylato)ruthenium(II) (N719 dye) in absolute ethanol for one day. The dye coated photoelectrode was washed, dried and immediately used for the measurement of solar cell performance. A sandwich type photoelectrochemical cell was used, which was composed of a dye-coated TiO_2 photoanode. Platinum coated fluorinated tin oxide (FTO) acted as a counter electrode. The electrolyte solution was injected into the space between photoanode and counter electrode. The electrolyte solution was composed of lithium iodide (LiI, 0.1 M); iodine (0.01 M), and dendrimer (0.1 mM) additives in 10 mL DMF solvent. The photovoltaic properties were measured under simulated solar light at 70 mWcm^{-2} . Current-voltage (J-V) measurement was performed using Metrohm Autolab 302N potentiostat/galvanostat with FRA32M module controlled by NOVA 1.10 software. The apparent cell area of the TiO_2 photoelectrode was 1 cm^2 (1 cm X 1 cm).

General procedure for zeroth generation dendrimers

A mixture of diyne **25** and triyne **26** (1.0 equiv.) and 2-(4-(azidomethyl)phenyl)benzoheterazole **13** and **14** (2.2 equiv./ 3.3 equiv.) was dissolved in a mixture of THF and H₂O (1:1; 20 mL) and sodium ascorbate (10 mol%) was added followed by the addition of CuSO₄·5H₂O (5 mol%). The reaction mixture was stirred overnight at room temperature. The residue obtained after evaporation of the solvent was washed thoroughly with water and dissolved in CHCl₃ (3 x 100 mL). The organic layer was washed with water (200 mL) and brine (50 mL), dried over Na₂SO₄, and then solvent was evaporated to give the crude triazole product, which was purified by column chromatography (SiO₂) with CHCl₃ or CHCl₃-MeOH as eluent to give the corresponding triazole dendrimers.

Dendrimer 1

Yield: 65%; mp: 250-254 °C; ¹H NMR (300 MHz, CDCl₃): δ_H 5.60 (s, 4H); 7.05 (s, 2H); 7.10 (d, *J* = 2.4 Hz, 4H); 7.13 (s, 3H); 7.26 (d, *J* = 15.6 Hz, 2H); 7.33 (d, *J* = 7.5 Hz, 8H); 7.53 (t, *J* = 5.1 Hz, 2H); 7.60 (d, *J* = 8.1 Hz, 4H); 7.63 (s, 2H); 7.67 (d, *J* = 8.7 Hz, 2H); 7.71 (t, *J* = 4.2 Hz, 3H); 7.77 (d, *J* = 16.5 Hz, 2H). ¹³C NMR (75 MHz, CDCl₃): δ_C 53.8, 109.0, 110.3, 114.9, 118.9, 123.4, 124.0, 124.6, 124.7, 124.8, 125.4, 126.7, 128.1, 128.5, 129.4, 135.7, 136.2, 138.2, 142.1, 147.1, 147.5, 148.1, 150.4, 162.4. ESI-MS *m/z* 846 [M + H]⁺. Anal. Calcd. for C₅₄H₃₉N₉O₂: C, 76.67; H, 4.65; N, 14.90. Found: C, 75.68; H, 4.73; N, 14.79%.

Dendrimer 2

Yield: 70%; mp: 258-260 °C; ¹H NMR (300 MHz, CDCl₃): δ_H 5.59 (s, 4H); 7.04 (t, *J* = 7.2 Hz, 1H); 7.11 (d, *J* = 8.7 Hz, 6H); 7.26 (d, *J* = 15.6 Hz, 4H); 7.33 (d, *J* = 7.8 Hz, 4H); 7.36 (s, 1H); 7.43 (t, *J* = 7.5 Hz, 3H); 7.52 (d, *J* = 11.1 Hz, 3H); 7.59 (d, *J* = 8.1 Hz, 4H); 7.63 (s, 2H);

7.68 (d, $J = 8.4$ Hz, 4H); 7.86 (d, $J = 7.8$ Hz, 2H); 8.00 (d, $J = 8.1$ Hz, 2H). ^{13}C NMR (75 MHz, CDCl_3): δ_{c} 53.8, 118.9, 121.5, 123.0, 123.1, 124.0, 124.7, 124.8, 125.5, 126.4, 126.7, 128.0, 128.5, 129.4, 129.4, 134.4, 135.8, 135.9, 136.4, 147.1, 147.5, 148.1, 153.8, 166.5. ESI-MS m/z 878 $[\text{M} + \text{H}]^+$. Anal. Calcd. for $\text{C}_{54}\text{H}_{39}\text{N}_9\text{S}_2$: C, 73.86; H, 4.48; N, 14.36. Found: C, 73.76; H, 4.56; N, 14.28%.

Dendrimer 5

Yield: 60%; mp: 252-254 $^{\circ}\text{C}$; ^1H NMR (300 MHz, CDCl_3): δ_{H} 5.62 (s, 6H); 7.13 (d, $J = 8.7$ Hz, 7H); 7.36 (d, $J = 7.8$ Hz, 12H); 7.43 (s, 2H); 7.54 (t, $J = 4.5$ Hz, 3H); 7.61 (d, $J = 8.1$ Hz, 6H); 7.72 (t, $J = 8.4$ Hz, 11H); 7.80 (s, 3H). ^{13}C NMR (75 MHz, $\text{DMSO}-d_6$): δ_{c} 52.6, 108.1, 110.5, 114.2, 119.5, 121.1, 124.0, 124.7, 125.5, 126.5, 128.2, 128.3, 134.6, 137.6, 138.7, 141.6, 146.3, 146.4, 149.7, 162.2. ESI-MS m/z 1146 $[\text{M} + \text{H}]^+$. Anal. Calcd. for $\text{C}_{72}\text{H}_{51}\text{N}_{13}\text{O}_3$: C, 75.44; H, 4.48; N, 15.89. Found: C, 75.53; H, 4.40; N, 15.76%.

Dendrimer 6

Yield: 67%; mp: 230-232 $^{\circ}\text{C}$; ^1H NMR (300 MHz, CDCl_3): δ_{H} 5.45 (s, 6H); 6.99 (d, $J = 8.4$ Hz, 6H); 7.19 (d, $J = 8.4$ Hz, 6H); 7.25 (d, $J = 6$ Hz, 2H); 7.29 (s, 3H); 7.34 (d, $J = 3.9$ Hz, 6H); 7.49 (d, $J = 7.8$ Hz, 6H); 7.57 (d, $J = 4.5$ Hz, 10H); 7.53 (d, $J = 7.8$ Hz, 3H); 7.88 (d, $J = 8.1$ Hz, 3H). ^{13}C NMR (75 MHz, $\text{DMSO}-d_6$): δ_{c} 52.7, 118.2, 120.5, 121.9, 122.0, 123.3, 124.2, 124.4, 125.3, 125.7, 126.9, 127.4, 133.3, 134.8, 135.0, 135.3, 146.1, 146.9, 152.7, 165.4. ESI-MS m/z 1194 $[\text{M} + \text{H}]^+$. Anal. Calcd. for $\text{C}_{72}\text{H}_{51}\text{N}_{13}\text{S}_3$: C, 72.40; H, 4.30; N, 15.24. Found: C, 72.290; H, 4.23; N, 15.29%.

General procedure for first generation dendrimers

A mixture of diyne **25** and triyne **26** (1.0 equiv.) and dendritic azide **19** and **20** (2.2 equiv. /3.3 equiv.) was dissolved in a mixture of DMF and H₂O (4:1; 20 mL) and sodium ascorbate (10 mol%) was added followed by the addition of CuSO₄·5H₂O (5 mol%). The reaction mixture was stirred for 24 h at room temperature. The reaction mixture was poured with water (200 mL) and dissolved in CHCl₃ (3 x 100 mL). The organic layer was separated and then washed with water (200 mL) and brine (50 mL), dried over Na₂SO₄, and evaporated to give the corresponding dendrimers, which was purified by column chromatography (SiO₂) using CHCl₃: MeOH as the eluent.

Dendrimer 3

Yield: 58%; mp: 216-220 °C; ¹H NMR (300 MHz, DMSO-d₆): δ_H 5.12 (s, 8H); 5.53 (s, 4H); 5.62 (s, 8H); 6.60 (s, 4H); 6.72 (s, 4H); 7.02 (d, *J* = 7.5 Hz, 6H); 7.34 (d, *J* = 7.8 Hz, 22H); 7.72 (m, 23H); 8.30 (s, 6H); 8.53 (s, 2H). ¹³C NMR (75 MHz, CDCl₃): δ_c 52.5, 61.5, 79.5, 101.0, 107.1, 114.2, 119.5, 121.0, 123.6, 124.2, 124.7, 124.8, 125.1, 125.5, 126.4, 128.2, 128.4, 129.5, 134.6, 137.4, 138.1, 138.7, 141.6, 142.7, 146.3, 146.5, 149.7, 159.3, 162.1. ESI-MS *m/z* 1881 [*M* + H]⁺. Anal. Calcd. for C₁₁₂H₈₅N₂₃O₈: C, 71.51; H, 4.55; N, 17.13. Found: C, 71.40; H, 4.63; N, 17.09%.

Dendrimer 4

Yield: 53%; mp: 220-222 °C; ¹H NMR (300 MHz, DMSO-d₆): δ_H 3.90 (s, 8H); 4.31 (s, 4H); 4.39 (s, 8H); 5.38 (s, 4H); 5.50 (s, 2H); 5.80 (d, *J* = 7.8 Hz, 6H); 6.04 (d, *J* = 7.5 Hz, 2H); 6.11 (d, *J* = 7.8 Hz, 9H); 6.18 (t, *J* = 7.5 Hz, 5H); 6.26 (d, *J* = 7.8 Hz, 5H); 6.38 (s, 6H); 6.52 (d, *J* = 7.8 Hz, 12H); 6.71 (d, *J* = 8.1 Hz, 4H); 6.82 (d, *J* = 7.8 Hz, 4H); 7.06 (s, 4H); 7.30 (s, 2H).

^{13}C NMR (75 MHz, DMSO- d_6): δ_c 52.5, 52.9, 61.1, 101.1, 107.1, 121.0, 122.1, 122.2, 122.5, 123.6, 124.2, 124.7, 125.1, 125.4, 126.4, 126.5, 128.0, 128.4, 129.5, 134.0, 135.0, 136.6, 137.0, 138.1, 142.7, 146.3, 146.5, 146.7, 153.3, 159.3, 166.2. ESI-MS m/z 1967 $[\text{M} + \text{Na}]^+$. Anal.Calcl.for $\text{C}_{112}\text{H}_{85}\text{N}_{23}\text{O}_4\text{S}_4$: C, 69.15; H, 4.40; N, 16.56. Found: C, 69.27; H, 4.33; N, 15.64%.

Dendrimer 7

Yield: 55%; mp: 158-162 °C; ^1H NMR (300 MHz, DMSO- d_6): δ_H 5.12 (s, 12H); 5.54 (s, 6H); 5.62 (s, 12H); 6.61 (s, 6H); 6.72 (s, 3H); 6.92 (d, $J = 8.7$ Hz, 2H); 7.06 (t, $J = 8.4$ Hz, 6H); 7.26 (d, $J = 3.9$ Hz, 3H); 7.34 (d, $J = 7.8$ Hz, 25H); 7.67 (m, 12H); 7.75 (m, 24H); 8.30 (s, 6H); 8.56 (s, 3H). ^{13}C NMR (75 MHz, DMSO- d_6): δ_c 52.5, 61.1, 79.1, 101.0, 107.2, 110.5, 114.2, 119.5, 124.6, 124.8, 125.4, 126.4, 126.5, 128.2, 128.4, 130.2, 134.7, 137.4, 138.1, 138.6, 141.6, 142.7, 145.8, 146.2, 146.3, 149.7, 159.3, 162.1. ESI-MS m/z 2699 $[\text{M} + \text{H}]^+$. Anal.Calcl.for $\text{C}_{159}\text{H}_{120}\text{N}_{34}\text{O}_{12}$: C, 70.16; H, 4.48; N, 17.65. Found: C, 70.06; H, 4.57; N, 17.56%.

Dendrimer 8

Yield: 50%; mp: 188-192 °C; ^1H NMR (300 MHz, DMSO- d_6): δ_H 5.13 (s, 12H); 5.54 (s, 6H); 5.61 (s, 12H); 6.61 (s, 6H); 6.72 (s, 3H); 7.05 (d, $J = 8.4$ Hz, 6H); 7.32 (d, $J = 8.1$ Hz, 12H); 7.39 (t, $J = 7.8$ Hz, 5H); 7.49 (t, $J = 7.5$ Hz, 6H); 7.59 (s, 10H); 7.74 (d, $J = 8.1$ Hz, 18H); 7.93 (d, $J = 8.1$ Hz, 6H); 8.02 (d, $J = 7.8$ Hz, 6H); 8.29 (d, $J = 4.5$ Hz, 9H); 8.53 (s, 3H). ^{13}C NMR (75 MHz, DMSO- d_6): δ_c 52.5, 61.1, 79.0, 101.0, 107.2, 121.0, 122.0, 122.2, 122.5, 122.6, 124.0, 124.7, 125.4, 126.4, 128.0, 128.4, 129.3, 134.0, 135.0, 135.2, 136.6, 137.0, 138.1, 142.7, 146.3, 153.3, 159.3, 166.2. ESI-MS m/z 2817 $[\text{M} + \text{Na}]^+$. Anal.Calcl.for $\text{C}_{159}\text{H}_{120}\text{N}_{34}\text{O}_6\text{S}_6$: C, 68.32; H, 4.33; N, 17.04. Found: C, 68.44; H, 4.27; N, 17.15%.

Acknowledgments

The authors thank UGC, New Delhi, India, for financial support and DST-FIST for providing NMR facilities to the Department of Organic Chemistry, University of Madras, Chennai, India and Dr. V. Subramanian, Chemical laboratory, CSIR-CLRI, Chennai for molecular orbital calculations and High Performance Computing Environment (HPCE) facility at IIT Madras for DFT and DSSC measurements. KR thanks University of Madras for University Research Fellowship (URF).

References

1. J. Yang, D. Yan, and T. S. Jones, *Chem. Rev.*, 2015, **115**, 5570–5603.
2. S. R. Forrest and M. E. Thompson, *Chem. Rev.*, 2007, **107**, 923-925.
3. S. -H. Hwang, C. N. Moorefield and G. R. Newkome, *Chem. Soc. Rev.*, 2008, **37**, 2543-2557.
4. (a) E. Buhleier, W. Wehner and F. Vogtle, *Synthesis*, 1978, **2**, 155-158. (b) C. J. Hawker, J. M. J. Frechet and D. A. Tomalia, John Wiley & Sons, Ltd, Chichester, 2001, 1-1072. (c) C. J. Hawker and J.M. J. Frechet, *J. Am. Chem. Soc.*, 1990, **112**, 7638-7647. (d) G. R. Newkome, Z. Yao, G. R. Baker and V. K. Gupta, *J. Org. Chem.*, 1985, **50**, 2003-2004.
5. S. Svenson, *Eur. J. Pharm. Biopharm.*, 2009, **71**, 445-462.
6. P. Rajakumar, V. Kalpana, S. Ganesan and P. Maruthamuthu, *New J. Chem.*, 2013, **37**, 3692-3700.
7. V. Balzani, G. Bergamini, P. Ceroni and E. Marchi, *New J. Chem.*, 2011, **35**, 1944-1954.
8. L. -P. Wu, M. Ficker, J. B. Christensen, P. N. Trohopoulos, and S. M. Moghimi, *Bioconjugate Chem.*, 2015, **26**, 1198–1211.
9. E. Ay, S. Furukawa and E. Nakamura, *Org. Chem. Front.*, 2014, **1**, 988–991.

10. (a) R. Misra, R. Maragani, K. R. Patel and G. D. Sharma, *RSC Adv.*, 2014, **4**, 34904-34911. (b) W. Xu, B. Peng, J. Chen, M. Liang and F. Cai, *J. Phys. Chem. C*, 2008, **112**, 874-880. (c) Y. Liang, B. Peng and J. Chen, *J. Phys. Chem. C*, 2010, **114**, 10992-10998.
11. (a) T. -T. Bui, L. Beouch, X. Sallenave, F. Goubard, *Tetrahedron Letters*, 2013, **54**, 4277-4280. (b) Y. Shiota, *J. Mater. Chem.*, 2005, **15**, 75-93.
12. T. Shoji, S. Ito, T. Okujima and N. Morita, *Org. Biomol. Chem.*, 2012, **10**, 8308-8318.
13. (a) E. Ripaud, Y. Olivier, P. Leriche, J. Cornil and J. Roncali, *J. Phys. Chem. B*, 2011, **115**, 9379-9386. (b) C. Fan, X. Wang, P. Ding, J. Wang, Z. Liang and X. Tao, *Dyes Pigment.*, 2012, **95**, 757-767.
14. (a) Z. Wu, X. Li, J. Li, H. Agren, J. Hua and H. Tian, *J. Mater. Chem. A*, 2015, **3**, 14325-14333. (b) A. N. -Król, R. Wagener, F. Kraus, A. Mishra, P. Bäuerle and F. Würthner, *Org. Chem. Fron.*, **2016**, DOI: 10.1039/c6qo00046k.
15. H. Kusama, H. Orita and H. Sugihara, *Langmuir*, 2008, **24**, 4411-4419.
16. B. O'Regan and M. Gratzel, *Nature*, 1991, **353**, 737-740.
17. (a) V. Kalpana, K. Rajavelu and P. Rajakumar, *Aust. J. Chem.*, 2015, **68**, 93-98. (b) P. Rajakumar and V. Kalpana, *RSC Adv.*, 2014, **4**, 3782-3788.
18. (a) C. A. Mathis, Y. Wang, D. P. Holt, G. F. Huang, M. L. Debnath and W. E. Klunk, *J. Med. Chem.*, 2003, **46**, 2740-2754. (b) I. Hutchinson, A. S. Jenninga, B. R. Vishnuvajjala, A. D. Westwell and M. F. G. Stevens, *J. Med. Chem.*, 2002, **45**, 744-747. (c) R. Caujolle, P. Loiseau, M. Payard and P. Gayral, *Ann. Pharm. Fr.*, 1989, **47**, 68-73. (d) K. Yamamoto, M. Fujita, K. Tabashi, Y. Kawashima, E. Kato, M. Oya, J. Iso and T. Iwao, *J. Med. Chem.*, 1998, **31**, 919-930. (e) H. Yoshida, R. Nakao, H. Nohta and M.

- Yamaguchi, *Dyes Pigments*, 2000, **47**, 239-245. (f) I. Petkov, T. Deligeorgiev, P. Markov, M. Evstatiev and S. Fakirov, *Polym. Degrad. Stab.*, 1991, **33**, 53-66.
19. (a) P. Rajakumar, V. Kalpana, S. Ganesan and P. Maruthamuthu, *Tetrahedron Lett.*, 2011, **52**, 5812-5816. (b) P. Rajakumar, C. Satheeshkumar, M. Ravivarma, S. Ganesan and P. Maruthamuthu, *J. Mater. Chem. A*, 2013, **1**, 13941-13948.
20. S. Raja, C. Satheeshkumar, P. Rajakumar, S. Ganesan and P. Maruthamuthu, *J. Mater. Chem.*, 2011, **21**, 7700-7704.
21. P. Rajakumar, K. Visalakshi, S. Ganesan. P. Maruthamuthu and S. Austin suthanthiraraj, *Aust. J. Chem.*, 2011, **64**, 951-956.
22. F. A. S. Chipem, S. Chatterjee and G. Krishnamoorthy, *Journal of Photochemistry and Photobiology A: Chemistry*, 2010, **214**, 121-127.
23. M. Mba, M. D'Acunzo, P. Salice, T. Carofiglio, M. Maggini, S. Caramori, A. Campana, A. Aliprandi, R. Argazzi, S. Carli and C. A. Bignozzi, *J. Phys. Chem. C*, 2013, **117**, 19885-19896.
24. T. A. Fayed and S. S. Ali, *SPECTROSCOPY LETTERS*, 2003, **36**, 375-386.
25. S. K. Saha, P. Purkayastha and A. B. Das, *J. Photochem. Photobiol. A: Chem.*, 2008, **195**, 368-377.
26. T. H. Kwon, M. K. Kim, J. Kwon, T. Y. Shin, S. J. Park, C. L. Lee, J. J. Kim and J. I. Hong, *Chem. Mater.*, 2007, **19**, 3673-3680.
27. M. -H. Tremblay, T. Skalski, Y. Gautier, G. Pianezzola and W. G. Skene, *J. Phys. Chem. C*, 2016, **120**, 9081-9087.
28. K. Onitsuka, N. Ohara, F. Takei and S. Takahashi, *Dalton Trans.*, 2006, 3693-3698.

29. (a) A.D. Becke, *J. Chem. Phys.*, 1993, **98**, 5648-5652. (b) C. Lee, W. Yang and R.G. Parr, *Phys. Rev. B*, 1988, **37**, 785-789.
30. (a) T. Duan, K. Fan, Y. Fu, C. Zhong, X. Chen, T. Peng and J. Qin, *Dyes and Pigments*, 2012, **94**, 28-33. (b) P. Brogdon, L. E. McNamara, A. Peddapuram, N. I. Hammer, J. H. Delcamp, *Synthetic Met.*, **2016**, DOI: 10.1016/j.synthmet.2016.03.031.
31. B. -K. An, R. Mulherin, B. Langley, P. Burn and P. Meredith, *Organic Electronics*, **2009**, **10**, 1356-1363.
32. T. Sudyoadsuk, S. Pansay, S. Morada, R. Rattanawan, S. Namuangruk, T. Kaewin, S. Jungsuttiwong and V. Promarak, *Eur. J. Org. Chem.*, **2013**, 5051–5063.
33. Y. J. Chang, P. -T. Chou, S. -Y. Lin, M. Watanabe, Z.-Q. Liu, J. -L. Lin, K. -Y. Chen, S. -S. Sun, C. -Y. Liu, and T. J. Chow, *Chem. Asian J.* 2012, **7**, 572-581.
34. S. A. Ponomarenko, Y. N. Luponosov, J. Min, A. N. Solodukhin, N. M. Surin, M. A. Shcherbina, S. N. Chvalun, T. Americ and C. Brabec, *Faraday Discuss.*, 2014, **174**, 313-339.
35. (a) P. Thongkasee, A. Thangthong, N. Janthasing, T. Sudyoadsuk, S. Namuangruk, T. Keawin, S. Jungsuttiwong and V. Promarak, *ACS Appl. Mater. Interfaces*, 2014, **6**, 8212-8222. (b) W. -I. Hung, Y. -Y. Liao, C. -Y. Hsu, H. -H. Chou, T.-H. Lee, W. -S. Kao and J. T. Lin, *Chem. Asian J.* 2014, **9**, 357-366. (c) Y. Ooyama, K. Uenaka and J. Ohshita, *Org. Chem. Front.*, 2015, **2**, 552–559.
36. C. Sakong, S. H. Kim, S. B. Yuk, J. W. Namgoong, S. W. Park, M. J. Ko, D. H. Kim, K. S. Hong, and J. P. Kim, *Chem. Asian J.* 2012, **7**, 1817-1826. b) N. Satoh, T. Nakashima and K. Yamamoto, *J. Am. Chem. Soc.*, 2005, **127**, 13030-13038.

37. (a) T. N. Murakami, N. Koumura, E. Yoshida, T. Funaki, S. Takano, M. Kimura and S. Mori, *Langmuir*, 2016, **32**, 1178-1183. (b) S. Mathew, A. Yella, P. Gao, R. H. -Baker, B. F. E. Curchod, N. A. -Astani, I. Tavernelli, U. Rothlisberger, M. Khaja Nazeeruddin and Michael Gratzel, *nature chemistry*, **2014**, DOI: 10.1038/NCHEM.1861.
38. (a) A. Burke, S. Ito, H. Snaith, U. Bach, J. Kwiakowski and M. Grätzel, *Nano Lett.*, 2008, **8**, 977-981.
39. (a) A. N.-Krol, B. Fimmel, M. Son, D. Kim and F. Wurthner, *Faraday Discuss.*, 2015, **185**, 507-525.
40. H. Tian, X. Yang, R. Chen, R. Zhang, A. Hagfeldt and L. Sun, *J. Phys. Chem. C*, 2008, **112**, 11023-11033.
41. T. Pongsathorn, T. Amonrat, J. Nittaya, S. Taweesak, N. Supawadee, K. Tinnagon, J. Siriporn, and P. Vinich, *ACS Appl. Mater. Interfaces*, **2014**, 6, 8212-8222.
42. M. Cheng, X. Yang, J. Li, C. Chen, J. Zhao, Y. Wang and L. Sun, *Chem.-Eur. J.*, **2012**, 18, 16196-16202.
43. B. Hosseinzadeh, A. S. Beni, M. Azari, M. Zarandi and M. Karami, *New J. Chem.*, **2016**, 40, 8371-8381.
44. M. Cheng, X. Yang, J. Li, C. Chen, J. Zhao, Y. Wang, and L. Sun, *Chem. Eur. J.* **2012**, 18, 16196-16202.
45. S. P. Singh, M. S. Roy, K. R. Justin Thomas, S. Balaiah, K. Bhanuprakash and G. D. Sharma, *J. Phys. Chem. C*, 2012, **116**, 5941-5950.
46. A. Henning, G. Günzburger, R. Jöhr, Y. Rosenwaks, B. B. -Weber, C. E. Housecroft, E. C. Constable, E. Meyer and T. Glatzel, *Beilstein J. Nanotechnol.*, 2013, **4**, 418-428.

Graphical Abstract

Synthesis, photophysical, electrochemical and DSSC application of novel donor-acceptor triazole bridged dendrimers with triphenylamine core and benzoheterazole as surface unit

Kannan Rajavelu,^a Perumal Rajakumar,^{*a} Mandal Sudip^b and Ramanujam Kothandaraman^b

Triazole bridged novel donor- acceptor dendrimers were synthesized via click chemistry. Lower generation dendrimers when used as additives exhibit better current generating capacity and power conversion efficiency in DSSCs.

